



Preparation of ferroelectric BaTi₂O₅ thin films on Pt(1 1 1)/Ti/SiO₂/Si substrates by pulsed laser deposition

Junjun Wang, Chuanbin Wang*, Qiang Shen, Lianmeng Zhang

State Key Lab of Advanced Technology for Materials Synthesis and Processing, Wuhan University of Technology, Wuhan 430070, China

ARTICLE INFO

Article history:

Received 2 June 2011

Received in revised form

16 September 2011

Accepted 19 September 2011

Available online 22 September 2011

Keywords:

BaTi₂O₅ thin films

b-Axis orientation

Pulsed laser deposition

Pt(1 1 1)/Ti/SiO₂/Si substrates

Ferroelectric property

ABSTRACT

Ferroelectric BaTi₂O₅ thin films were prepared on Pt(1 1 1)/Ti/SiO₂/Si substrates by pulsed laser deposition under different substrate temperatures ($T_{\text{sub}} = 923\text{--}973\text{ K}$) and oxygen partial pressures ($P_{\text{O}_2} = 7.5\text{--}15\text{ Pa}$). The effects of T_{sub} and P_{O_2} on the phase, orientation and surface morphology of the as-deposited films were investigated. It was found that the crystallographic orientation of BaTi₂O₅ thin films strongly depended on T_{sub} and P_{O_2} . The BaTi₂O₅ film with the highest (0 2 0)-texture coefficient ($TC_{(020)} = 0.78$) was obtained at $T_{\text{sub}} = 943\text{ K}$ and $P_{\text{O}_2} = 12.5\text{ Pa}$, showing a higher degree of *b*-axis orientation as compared with those deposited under other parameters. The ferroelectric property of the BaTi₂O₅ thin films was then investigated and the polarization–electric field (*P*–*E*) loop was measured for the first time. The room temperature remanent polarization and coercive electric field of the BaTi₂O₅ thin film with a higher degree of *b*-axis orientation were $0.77 \times 10^{-2}\text{ C m}^{-2}$ and $1 \times 10^6\text{ V m}^{-1}$, respectively.

© 2011 Elsevier B.V. All rights reserved.

1. Introduction

Ferroelectric thin films have attracted much attention due to the potential applications in high density dynamic random access memories (DRAMs), non-volatile ferroelectric random access memories (FRAMs), microelectro-mechanical system (MEMS), microelectronics and optoelectronic devices [1,2]. In particular, BaTiO₃, PbTiO₃ and PbZr_{1-x}Ti_xO₃ have been extensively studied for their high dielectric constant and significant ferroelectricity [3–8]. However, these materials have drawbacks of low Curie temperature for BaTiO₃ ($T_C \approx 403\text{ K}$) and environmentally unfriendly element (Pb) contained in PbTiO₃ and PbZr_{1-x}Ti_xO₃. The development of new lead-free ferroelectric materials is required from the viewpoint of the protection of environment and the availability at higher temperatures.

As a TiO₂-rich phase in the BaO–TiO₂ system, BaTi₂O₅ is attracting attention recently, which was found to be a candidate for non-lead ferroelectric materials used in FRAMs or DRAMs and showed significant permittivity and ferroelectricity along *b*-axis direction [9,10]. Up to now, only Wang et al. [11–14] had prepared BaTi₂O₅ thin films on MgO(1 0 0) substrates by pulsed laser deposition, but the ferroelectricity of the films was not reported. In order to realize the application of BaTi₂O₅ thin films in ferroelectric devices, Pt(1 1 1)/Ti/SiO₂/Si substrates should be further employed

since they are commonly used bottom electrodes in current semiconductor technology due to the high electrical conductivity, low leakage current and good stability in high temperature oxidizing environments. In the present study, ferroelectric BaTi₂O₅ thin films with a higher degree of *b*-axis orientation were firstly prepared on Pt(1 1 1)/Ti/SiO₂/Si substrates by pulsed laser deposition. We herein report the effects of substrate temperature and oxygen partial pressure on the phase, orientation and surface morphology of the films. The ferroelectric property of the BaTi₂O₅ thin films was also investigated.

2. Experimental procedures

BaTi₂O₅ thin films were prepared on Pt(1 1 1)/Ti/SiO₂/Si substrates by pulsed laser deposition (PLD, PLVD-362). A Q-switch pulsed Nd: YAG laser with a wavelength of 355 nm and a repetition frequency of 10 Hz was used. The laser beam was introduced in to a deposition chamber at an angle of 45° and focused on a rotating target at an energy density of 3 J/cm². A spark plasma sintered BaTi₂O₅ ceramic disc with a relative density of 95% was used as the target. Pt(1 1 1)/Ti/SiO₂/Si substrate was placed parallel to the target at a distance of 50 mm. The chamber was evacuated to a high vacuum ($1 \times 10^{-6}\text{ Pa}$) and then the deposition was carried out under different oxygen partial pressures (P_{O_2}) up to 15 Pa for 4 h. The substrate temperature (T_{sub}) was changed from 923 K to 973 K. The deposition rate was 125 nm/h approximately.

The crystal structure of the films was identified by X-ray diffractometer (XRD, Rigaku Ultima III) with Cu α radiation. The Raman shift from a laser (785 nm) was measured by a Raman microscopy (Renishaw Invia) to identify the structure. The cross-section of the BaTi₂O₅ thin films was observed by a field emission scanning electron microscopy (FESEM, Hitachi S-4800). The surface morphology was measured by an atomic force microscopy (DI Nanoscope IV). The electric hysteresis loop of the films at room temperature was measured by a ferroelectric test system (Radiant, Precision Premier II). For ferroelectric property measurement, Pt circular top

* Corresponding author.

E-mail addresses: wondream@126.com, wangcb@whut.edu.cn (C. Wang).

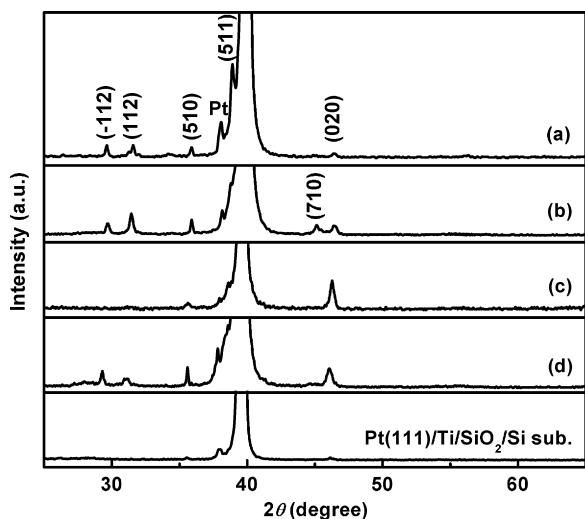


Fig. 1. XRD patterns of the films deposited on Pt(111)/Ti/SiO₂/Si substrates at $T_{\text{sub}} = 943$ K and $P_{\text{O}_2} =$ (a) 7.5 Pa, (b) 10 Pa, (c) 12.5 Pa and (d) 15 Pa. The pattern of Pt(111)/Ti/SiO₂/Si substrate is presented for comparison.

electrodes of 5×10^{-4} m in diameter were deposited on BaTi₂O₅ thin films at 200 °C by d.c. magnetron sputtering through a shadow mask.

3. Results and discussion

Fig. 1 shows the X-ray diffraction (XRD) patterns of the films deposited on Pt(111)/Ti/SiO₂/Si substrates at $T_{\text{sub}} = 943$ K under different oxygen partial pressures (P_{O_2}) from 7.5 Pa to 15 Pa. The XRD pattern of Pt(111)/Ti/SiO₂/Si substrate is also presented for comparison. Single-phased BaTi₂O₅ thin films were obtained at $P_{\text{O}_2} = 7.5$ –15 Pa. At $P_{\text{O}_2} = 7.5$ Pa, the diffraction peaks indexed to BaTi₂O₅ (-112), (112), (510), (511), (710), and (020) planes coexisted. With increasing P_{O_2} to 12.5 Pa, the (020)-oriented peak became stronger and sharper whereas other peaks were weakened. Further increasing P_{O_2} to 15 Pa, similar diffraction patterns as Fig. 1a appeared again.

However, XRD could not be informative to identify the second phase in the BaTi₂O₅ films since only several diffraction peaks were observed in Fig. 1 due to orientation growth. On the other hand, the Raman spectroscopy is independent of preferred orientation, and can be useful to assist the identification of crystal phase. Fig. 2 shows the Raman spectra of the films prepared at

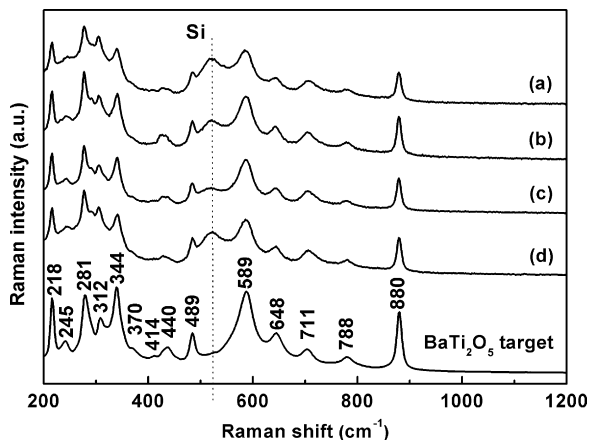


Fig. 2. Raman spectra of the films deposited on Pt(111)/Ti/SiO₂/Si substrates at $T_{\text{sub}} = 943$ K and $P_{\text{O}_2} =$ (a) 7.5 Pa, (b) 10 Pa, (c) 12.5 Pa and (d) 15 Pa. The spectrum of BaTi₂O₅ ceramic target is presented for comparison.

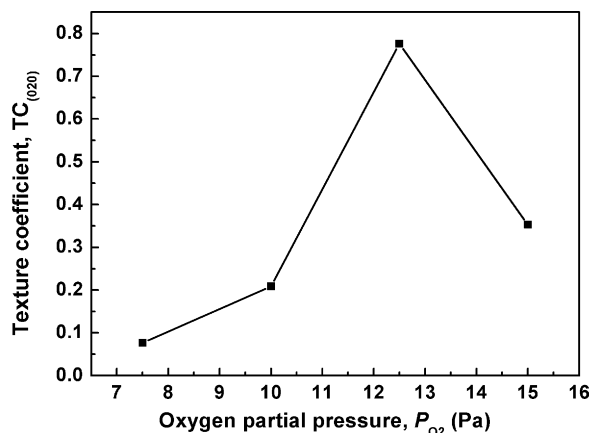


Fig. 3. $TC_{(020)}$ of the BaTi₂O₅ films deposited on Pt(111)/Ti/SiO₂/Si substrates at $T_{\text{sub}} = 943$ K as a function of P_{O_2} .

$T_{\text{sub}} = 943$ K and $P_{\text{O}_2} = 7.5$ Pa, 10 Pa, 12.5 Pa and 15 Pa, respectively. The Raman spectrum of the BaTi₂O₅ ceramic target used for film deposition is also depicted as comparison. Two stronger bands (344 and 589 cm⁻¹) and other bands (218, 245, 281, 312, 370, 414, 440, 489, 648, 711, 788, 880 cm⁻¹) indexed to BaTi₂O₅ phase [15,16] were clearly observed. Except for the band of Si (521 cm⁻¹) from the substrate, almost all the bands of the films were in good agreement with those of the BaTi₂O₅ target, and no characteristic bands of other BaO–TiO₂ compounds, e.g., BaTiO₃ (515 cm⁻¹) and Ba₆Ti₁₇O₄₀ (630 cm⁻¹), were identified. Therefore, the Raman spectra further confirmed that the as-deposited films were in single BaTi₂O₅ phase.

Also as shown in Fig. 1, the crystallographic orientation of the BaTi₂O₅ thin films changed with oxygen partial pressures (P_{O_2}). The preferential growth orientation was then determined using a texture coefficient $TC_{(hkl)}$, which can be calculated using the following equation [17]:

$$TC_{(hkl)} = \frac{I_{(hkl)}/I_{0(hkl)}}{1/N \left[\sum I_{(hkl)}/I_{0(hkl)} \right]}$$

where, $TC_{(hkl)}$ is the texture coefficient of (hkl) plane, and the larger the $TC_{(hkl)}$, the stronger the preferred orientation of (hkl) plane, $I_{(hkl)}$ is the measured intensity of (hkl) plane, $I_{0(hkl)}$ is the corresponding recorded intensity in JCPDS data file and N is the number of preferential growth orientations. Fig. 3 shows the variation of texture coefficient $TC_{(020)}$ calculated from the above equation as a function of oxygen partial pressure. We can see that $TC_{(020)}$ shows the highest value of 0.78 at $P_{\text{O}_2} = 12.5$ Pa, indicating the strongest reflex along (020) plane, i.e., a higher degree of b -axis orientation as compared with those deposited under other parameters.

Fig. 4 shows the XRD patterns of the films deposited on Pt(111)/Ti/SiO₂/Si substrates at $P_{\text{O}_2} = 12.5$ Pa and $T_{\text{sub}} = 923$ –973 K. All the films showed single BaTi₂O₅ phase and the (020) peak existed. At $T_{\text{sub}} = 923$ K, only weak (020) peak appeared. As T_{sub} increased to 943 K, the orientation of the BaTi₂O₅ thin films changed from (511) to (020), but would change back to (511) at $T_{\text{sub}} > 943$ K.

Fig. 5 depicts the texture coefficient $TC_{(020)}$ of the BaTi₂O₅ films as a function of substrate temperature, which showed the highest value of 0.78 at $T_{\text{sub}} = 943$ K. Therefore, the appropriate substrate temperature to form BaTi₂O₅ films with a higher degree of b -axis orientation could be 943 K.

It can be found that the substrate temperature plays an important role in determining the structure of BaTi₂O₅ thin films. The change in the crystallographic orientation of the films with T_{sub} could be explained in terms of lattice mismatch, mobility of the

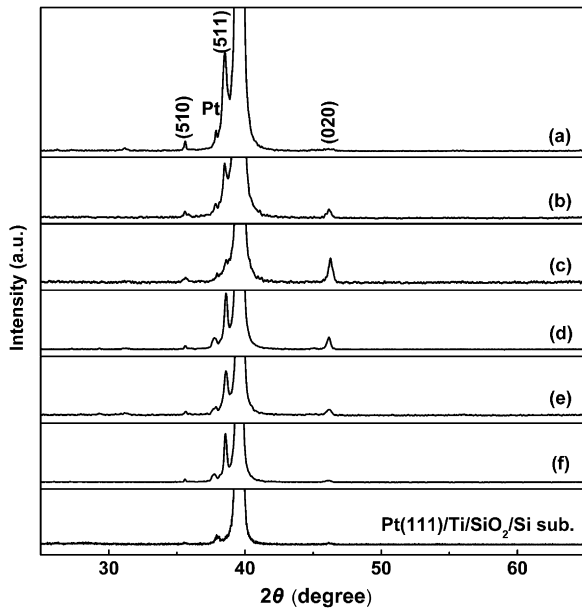


Fig. 4. XRD patterns of the films deposited on Pt(111)/Ti/SiO₂/Si substrates at $P_{O_2} = 12.5$ Pa and $T_{sub} =$ (a) 923 K, (b) 933 K, (c) 943 K, (d) 953 K, (e) 963 K and (f) 973 K. The pattern of Pt(111)/Ti/SiO₂/Si substrate is presented for comparison.

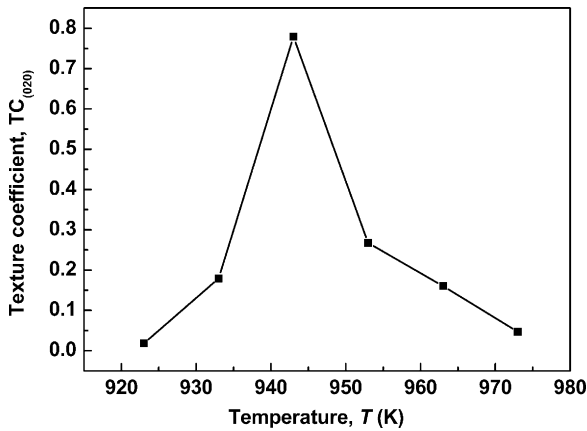


Fig. 5. $TC_{(020)}$ of the BaTi₂O₅ films deposited on Pt(111)/Ti/SiO₂/Si substrates at $P_{O_2} = 12.5$ Pa as a function of T_{sub} .

laser-ablated species and the surface energy of crystal planes. The low substrate temperature results in the weak surface migration of adatoms, so the growth orientation of the films will be influenced by the substrate's orientation to a great extent. For the BaTi₂O₅/Pt(111)/Ti/SiO₂/Si system, the (511) plane of BaTi₂O₅

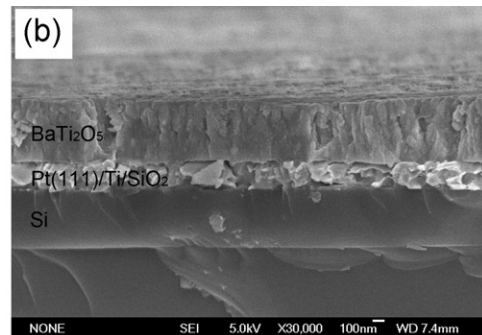
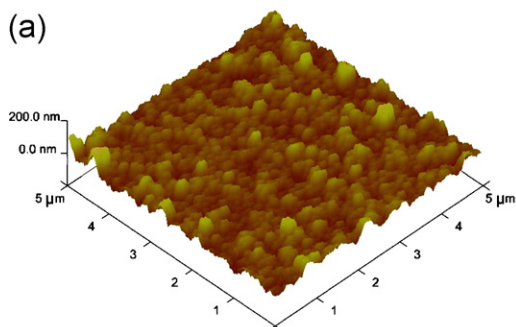


Fig. 6. (a) AFM image of surface morphology and (b) FESEM image of cross-section of BaTi₂O₅ thin film deposited on Pt(111)/Ti/SiO₂/Si at $T_{sub} = 943$ K and $P_{O_2} = 12.5$ Pa.

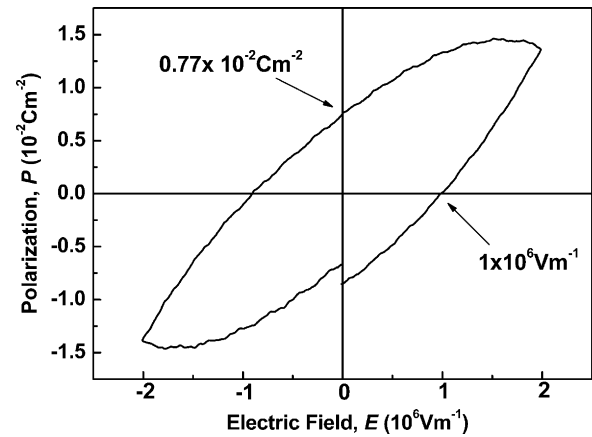


Fig. 7. Room temperature P - E loop of BaTi₂O₅ thin film deposited on Pt(111)/Ti/SiO₂/Si at $T_{sub} = 943$ K and $P_{O_2} = 12.5$ Pa.

with 2 unit cells and the (111) plane of Pt with 2 unit cells show similar dimensions and good matching. As compared with (020) and (510) planes, BaTi₂O₅ (511) exhibits the best matching with Pt(111). Therefore, the reflex peak of (511) plane appears as the strongest diffraction peak at low substrate temperatures. As T_{sub} increases, the ablated species have enough mobility to settle down at the stable plane to form the (020) orientation, which is one of the densest atomic-packing planes. But further increasing T_{sub} causes the adatoms to re-evaporate from the film surface, so there will be no enough adatoms to form the orientation of (020) plane.

Fig. 6 shows the images of surface morphology and cross-section of the BaTi₂O₅ thin film deposited on Pt(111)/Ti/SiO₂/Si substrate at $T_{sub} = 943$ K and $P_{O_2} = 12.5$ Pa, which were measured by the atomic force microscopy (AFM) and field emission scanning electron microscopy (FESEM), respectively. The film shows a relatively smooth and dense surface, and exhibits good adhesion to the substrate. The BaTi₂O₅ thin film is approximately 500 nm in thickness and fairly uniform.

Fig. 7 shows the room temperature ferroelectric property of the BaTi₂O₅ thin film with a higher degree of b -axis orientation, which was deposited on Pt(111)/Ti/SiO₂/Si substrate at $T_{sub} = 943$ K and $P_{O_2} = 12.5$ Pa. The polarization–electric field (P - E) loop was measured for the first time, and the remnant polarization and coercive electric field of the film were $0.77 \times 10^{-2} \text{ Cm}^{-2}$ and $1 \times 10^6 \text{ V m}^{-1}$, respectively. This was similar to BaTi₂O₅ single crystals, whose remnant polarization and coercive electric field at room temperature were $1.92 \times 10^{-2} \text{ Cm}^{-2}$ and $2.44 \times 10^5 \text{ V m}^{-1}$, respectively [10]. The little difference may be attributed to the existence of orientations other than (020) in the BaTi₂O₅ thin films because BaTi₂O₅ shows significant ferroelectricity only along b -axis direction.

4. Conclusions

Ferroelectric BaTi₂O₅ thin films were prepared on Pt(111)/Ti/SiO₂/Si substrates by pulsed laser deposition. The orientation of the films changed with increasing substrate temperature (T_{sub}) and oxygen partial pressure (P_{O_2}). The optimum conditions to obtain ferroelectric BaTi₂O₅ thin films were found to be $T_{\text{sub}} = 943 \text{ K}$ and $P_{\text{O}_2} = 12.5 \text{ Pa}$, where the (020) plane showed the highest texture coefficient ($\text{TC}_{(020)} = 0.78$), indicating a higher degree of *b*-axis orientation as compared with those deposited under other parameters. The room temperature remanent polarization and coercive electric field of the film were $0.77 \times 10^{-2} \text{ C m}^{-2}$ and $1 \times 10^6 \text{ V m}^{-1}$, respectively.

Acknowledgments

This work was financially supported by International Science and Technology Cooperation Project (2009DFB50470), National Natural Science Foundation of China (50802071) and International Science and Technology Cooperation Project of Hubei Province (2010BFA017).

References

- [1] J.F. Scott, C. Dearaujo, *Science* 246 (1989) 1400–1405.
- [2] M. Sayer, K. Sreenivas, *Science* 274 (1990) 1056.
- [3] S. Fuentes, R.A. Zarate, E. Chavez, et al., *J. Alloys Compd.* 509 (2010) 568–572.
- [4] Y.C. Lee, C.S. Chiang, *J. Alloys Compd.* 509 (2011) 6973–6979.
- [5] H.I. Hsiang, Y.L. Chang, J.S. Fang, F.S. Yen, *J. Alloys Compd.* 509 (2011) 7632–7638.
- [6] R. Wongmaneerung, S. Choopan, R. Yimnirun, S. Ananta, *J. Alloys Compd.* 509 (2011) 3547–3552.
- [7] L. Kerkache, A. Layadi, E. Dogheche, D. Remiens, *J. Alloys Compd.* 509 (2011) 6072–6076.
- [8] R. Frunza, D. Ricinschi, F. Gheorghiu, et al., *J. Alloys Compd.* 509 (2011) 6242–6246.
- [9] T. Akashi, H. Iwata, T. Goto, *Mater. Trans.* 44 (2003) 802–804.
- [10] T. Akashi, H. Iwata, T. Goto, *Mater. Trans.* 44 (2003) 1644–1646.
- [11] C.B. Wang, R. Tu, T. Goto, et al., *Mater. Chem. Phys.* 113 (2009) 130–134.
- [12] C.B. Wang, R. Tu, T. Goto, *J. Vac. Sci. Technol. A* 25 (2007) 304–307.
- [13] C.B. Wang, R. Tu, T. Goto, *Mater. Trans.* 48 (2007) 625–628.
- [14] C.B. Wang, R. Tu, T. Goto, et al., *J. Inorg. Mater.* 23 (2008) 553–556.
- [15] M. Rossel, H.R. Hoche, H.S. Leipner, et al., *Anal. Bioanal. Chem.* 380 (2004) 157–162.
- [16] A. Hushur, S. Kojima, *J. Korean Phys. Soc.* 46 (2005) 86–89.
- [17] P.S. Patil, P.S. Chigare, et al., *Mater. Chem. Phys.* 80 (2002) 667–675.